A Regulation Method Considering Coupled Voltage Violation and Unbalance in Three-Phase Four-Wire Hybrid AC/DC LVDNs with High Penetration PVs

Zhao, Chunxue; Li, Gen; Zhang, Lu; Zhang, Bo; Tang, Wei

Published in:
IEEE Transactions on Sustainable Energy

Link to article, DOI:
10.1109/TSTE.2023.3322317

Publication date:
2024

Document Version
Peer reviewed version

A Regulation Method Considering Coupled Voltage Violation and Unbalance in Three-Phase Four-Wire Hybrid AC/DC LVDNs with High Penetration PVs

Chunxue Zhao, *Student Member, IEEE*, Gen Li, *Senior Member, IEEE*, Lu Zhang, *Senior Member, IEEE*, Bo Zhang, *Member, IEEE* and Wei Tang, *Member, IEEE*

***Abstract*—Low-voltage distribution networks (LVDNs) have witnessed an increasing penetration of distributed photovoltaics (PVs), which exacerbates the existing voltage violation and voltage unbalance issues. PVs, energy storage systems, and voltage source converters can regulate voltages in hybrid AC/DC LVDNs. To solve the above two voltage problems simultaneously, a partition-based coordinated regulation method is proposed in this paper considering the coupling of the two issues and the effect of active power on reactive power in electrical distance calculation. The voltage adjustments in different voltage violation scenarios are obtained based on a graph that describes the coupling of the two issues mathematically. In order to better determine control devices, the equivalent coefficient of active power adjustment on electrical distance calculation is considered in the partition method, in which regulation efficiency, regulation cost, and regulation capability are used as objectives. The coordination of controllable devices is achieved according to three-phase four-wire sensitivities. Case studies are performed to verify the effectiveness and accuracy of the proposed regulation method in hybrid AC/DC LVDNs.**

***Index Terms*—Hybrid AC/DC LVDNs, coupled voltage violation and voltage unbalance, partition-based coordinated control, three-phase four-wire sensitivity**

I. Introduction

LOW-voltage distribution networks (LVDNs) are experiencing an increasing penetration of distributed photovoltaic (PV) [1]. However, the capacity-based single-phase or three-phase integration of PV can exacerbate voltage violation and voltage unbalance [2], [3]. For example, serious voltage violations and unbalances frequently and simultaneously occur in the Jinzhai power grid in Anhui Province, China due to the integration of about 40,000 household PV systems. Moreover, voltage violations may cause serious damage to electric equipment. Voltage unbalance may further aggravate power losses and threaten the security of system operation. Therefore, an effective control strategy for addressing the two issues is crucial for PV integration in LVDNs.

Various methods for improving voltage violations and unbalances have been studied in the literature. References [4]-[7] propose voltage control strategies through PV inverters, on-load tap changers, and energy storage systems (ESSs). However, they only study either voltage violation or voltage unbalance. It is known that the two issues always occur simultaneously as they are coupled. To address the two issues, [8] develops a priority-based voltage control strategy with voltage source converters (VSCs) in AC/DC LVDNs. [9] and [10] make comprehensive studies for optimizing voltage magnitude and balance profiles. An energy scheduling method is presented in [11] to mitigate voltage violation and voltage unbalance of a microgrid with a small cost. However, none of the above methods considers the coupling of the two issues and the global optimization in [9]-[11] is not justifiable for LVDNs with weak communication.

The coordination between PV inverters and ESS has been considered as a universal approach for voltage management in LVDNs [12]. Moreover, compared with AC systems, DC systems are more suitable for the integration of inverter-based PV systems and ESSs. VSC-based DC systems can provide better power qualities and flexible power control, thus the voltage unbalance can be mitigated through single-phase regulation of VSCs [13]. On the other hand, a hybrid AC/DC LVDN can mitigate overload and voltage violations due to the high-power transfer capacity of DC systems as well as the capability of power flow rescheduling [14]. Therefore, in hybrid AC/DC LVDNs, the coordination of controllable devices such as VSCs, ESSs, and PV inverters are suitable solutions for regulating voltage violations and unbalances. However, their coordinated regulation of active and reactive power still requires proper attention and solutions considering the three-phase four-wire structure on the AC side of a hybrid AC/DC LVDN.

To achieve efficient local control, [15] uses partitioning methods for voltage regulation. Compared to the global control method, the partition-based regulation method offers a simpler model with low computational burdens and allows separate voltage control in each sub-area. Local management of voltage violation and unbalance within the sub-area can prevent the issues from spreading to adjacent sub-areas and causing a wide impact. Therefore, compared to the above methods, the partition-based regulation method is more suitable for LVDNs with complex structures and multiple control devices. When the efficiencies of multiple devices are considered in a network

This work was supported by National Natural Science Foundation of China. (No. 51977211) (*Corresponding author: Lu Zhang)*

C. Zhao, L. Zhang, B. Zhang, and W. Tang are with China Agricultural University, Beijing 100083, China. (e-mail: caustuzcx@cau.edu.cn, zhanglu1@cau.edu.cn, zhangbo1223@foxmail.com, wei_tang@cau.edu.cn)

G. Li is with the Electric Energy Group, Department of Engineering Technology, Technical University of Denmark (DTU), 2750 Ballerup, Denmark. (email: genli@dtu.dk)

partition, it is necessary to define an electrical distance for calculating [16]. However, most existing methods only consider the effects of reactive power since they mainly focus on the reactive power partition of a balanced distribution network and voltage regulation in a transmission network, where the line resistance is much smaller than reactance [17]-[19]. [20] only calculates the electrical distance index of PVs based on active power-voltage sensitivity and reactive power-voltage sensitivity for voltage control in medium-voltage distribution networks (MVDNs). [21] presents a novel performance index based on electrical distance and regulation capability considering both active and reactive power of PV inverters to partition an MVDN. However, their control methods only regulate PV output. In [22], a novel partitioning method considering power balance and electric distance evaluated from active and reactive power sensitivity is proposed for voltage control in MVDNs.

However, unlike balanced MVDNs, the partition indexes calculation and sensitivity-based voltage control method are vulnerable to the three-phase four-wire structure of LVDNs. Furthermore, optimal control methods in [20]-[22] are unsuitable for LVDNs with weak communication.

Shortcomings of the existing coordinated control methods for addressing voltage violations and unbalances of hybrid AC/DC LVDNs include:

a) Voltage violations and voltage unbalances are solved separately or prioritized in most existing approaches. However, the regulation of phase voltage violation may worsen the voltage unbalance in three phases LVDNs, while voltage violation may also be further deteriorated by mitigating voltage unbalance. The reason is that the existing method of adjusting three-phase voltages to the average value increases the voltage deviation, due to the strong coupling between voltage violation and unbalance. Therefore, to address the two issues simultaneously, it is essential to consider and analyze them in a coordinated manner. Furthermore, a mathematical model is needed to explain and quantify the complex relationship between the two issues.

b) The three-phase structure and regulation capability of active power must be considered in the electrical distance calculation of hybrid AC/DC LVDNs. However, active power will be difficult to be embedded because the electrical distance parameters cannot be obtained. It is because that the comprehensive influence of active and reactive power is considered in the ratio of voltage deviation in the calculation of electrical distances. In this case, the reactive power in the numerator and denominator in the equation cannot be extracted and reduced as a coefficient.

c) Regulation effectiveness can be further improved considering the influence of the neutral line current in LVDNs on the other three phases. Moreover, the coupling between voltage violations and unbalances must be carefully embedded in the regulation method to effectively address the two issues simultaneously.

To tackle the aforementioned technical challenges, this paper proposes a coordinated regulation method for voltage violations and voltage unbalances considering the coupling of the two issues in hybrid AC/DC LVDNs. The specific contributions are summarized as follows:

a) A graph with quantifiable correlation derived from the three-phase analytical model is developed considering the coupling between voltage violations and unbalances. With the graph-based voltage regulation calculation method, voltage violation issues in LVDNs are explicitly classified into different scenarios, based on which the requirements of phase voltage control can be obtained in different scenarios to simultaneously address the two issues.

b) An equivalent coefficient is developed to consider the regulation efficiency of active power in the partition method of three-phase four-wire hybrid AC/DC LVDNs. Therefore, all of the regulation efficiency, cost, and capability of PV, ESSs, and VSCs are accurately considered to effectively determine the control devices in each partition.

c) A sensitivity method of hybrid AC/DC LVDNs is proposed considering the three-phase four-wire topology, based on which a coordinated regulation method for voltage violations and unbalances is proposed based on the developed graph for voltage regulation calculation and the control devices selected by the proposed partition method of hybrid AC/DC LVDNs.

II. Problem Description and Framework

Fig. 1 illustrates the structure of a hybrid AC/DC LVDN. AC side is a three-phase four-wire with a rated voltage of 220 V. DC side is a symmetrical monopole structure with metallic return and the DC rated voltage is ±375 V. Loads and PVs are connected in single-phase between the neutral wire. ESSs and VSCs are connected in three-phase on the AC side. Both active and reactive power outputs of PV inverters, ESSs, and VSCs are utilized for nodal voltage regulation.

Serious voltage violations such as over-voltage and under-voltage and unbalances can frequently and simultaneously occur on the AC side, which are exacerbated due to the increasing unbalanced distribution of distributed generation (e.g. PV). The DC side may face voltage violations because of the integration of single-phase grid-connection PV systems as shown in Fig. 1.

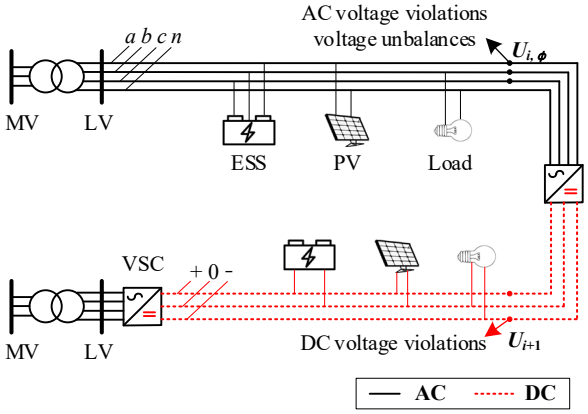

Fig. 1. Structure of a hybrid AC/DC LVDN.

As shown in Fig. 2, to solve voltage violation and unbalance simultaneously, a sensitivity-based coordinated control strategy

is proposed based on the partition method by coordinating multiple devices. The framework of the proposed control method is shown as follows:

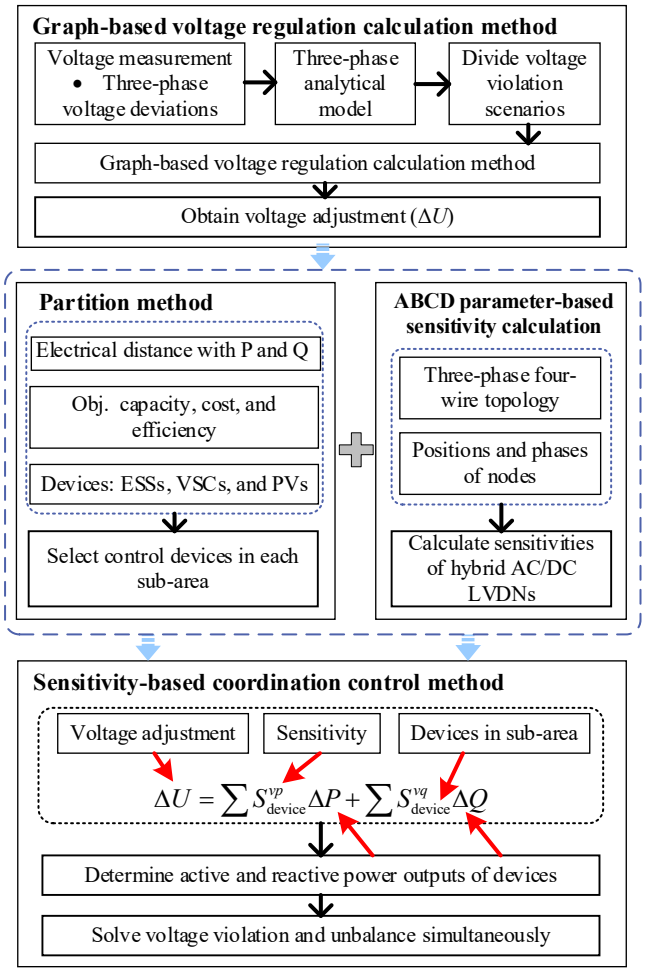

Fig. 2. The framework of the proposed coordinated control method.

a) Graph-Based Voltage Regulation Calculation Method. The coupling between voltage violation and unbalance is explained in Section III with the three-phase voltage deviations at a node. Then a graph-based voltage regulation calculation method is developed considering voltage violation scenarios and the coupling model, where voltage adjustment is obtained for solving the two issues simultaneously.

b) Partition Method and ABCD Parameter-Based Sensitivity Calculation. In Section IV-A, a partitioning method in three-phase four-wire hybrid AC/DC LVDNs is proposed considering the contributions of both active and reactive power on electrical distance calculation. The regulation efficiency, cost, and capability of ESSs, VSCs, and PVs are considered in the multi-objective functions of partition to determine the controllable devices in each sub-area. The optimal partition model is solved through a standard genetic algorithm in Section V. In Section IV-B, a power-voltage sensitivity calculation method is proposed by ABCD parameters for three-phase four-wire hybrid AC/DC LVDNs, considering different positions and phases of nodes. If the network configuration does not change, the sub-areas of LVDNs and the calculated active and reactive power-voltage sensitivity matrices will be constant and stored for use.

c) Sensitivity-Based Coordination Control Method. If a voltage issue occurs, the three-phase voltage adjustments will be obtained using a graph-based calculation method based on measured node voltages, and the partition method is utilized to identify the sub-area wherein the node is facing the voltage issue. Then the power outputs of controllable devices within this sub-area will be calculated based on the proposed sensitivity-based coordination control method of hybrid AC/DC LVDNs.

III. Graph-Based Voltage Adjustment Calculation Method

A. Three-phase Analytical Model of Coupled Voltage Violations and Unbalances

A three-phase analytical model using the three-phase voltage deviation as variables is proposed to identify the coupling between voltage violation and unbalance in AC LVDNs. The following is the derivation of the proposed coupling model.

The voltage deviations between the measured voltage and the rated voltage in hybrid AC/DC LVDNs as shown in Fig. 1 are:

$$\Delta U_i = U_i - U_{\text{rate, DC}}, \tag{1}$$

$$\Delta U_{i,\varphi} = U_{i,\varphi} - U_{\text{rate, AC}}, \tag{2}$$

where $U_{\text{rate, DC}}$ and $U_{\text{rate, AC}}$ are the rated per unit values of DC and AC LVDNs, $U_{\text{rate, DC}}$ = 1.0 p.u., $U_{\text{rate, AC}}$ = 1.0 p.u. and φ = *a*, *b*, and *c*. ΔU_i is 0.95 p.u. for under-voltage or 1.05 p.u. for over-voltage in DC LVDNs, while $\Delta U_{i,\varphi}$ is 0.93 p.u. for under-voltage or 1.07 p.u. for over-voltage in AC LVDNs.

Voltage unbalanced factor VU_i at node *i* of AC LVDNs, as shown in Fig. 1, is defined as follows

$$VU_{i,\varphi} = (\max\left|U_{i,\varphi} - U_i^{\text{avr}}\right|)/U_i^{\text{avr}} \times 100\%, \tag{3}$$

$$U_i^{\text{avr}} = (U_{i,a} + U_{i,b} + U_{i,c})/3, \tag{4}$$

where U_i^{avr} is the average voltage of three phases at node *i*. The parameter $VU_{i,\varphi}$ should not exceed the limit of 2% when the distribution network is in normal operation [24].

It is assumed that the phases of the maximum absolute value of $\Delta U_{i,\varphi}$ and the maximum $VU_{i,\varphi}$ are both in phase *a*. Thus, (5) can be obtained from (3):

$$VU_{i,a} = \frac{\max\left|\left[(\Delta U_{i,a} + U_{\text{rate,AC}}) - ((\Delta U_{i,a} + \Delta U_{i,b} + \Delta U_{i,c})/3 + U_{\text{rate,AC}})\right]\right|}{(\Delta U_{i,a} + \Delta U_{i,b} + \Delta U_{i,c})/3 + U_{\text{rate,AC}}}. \tag{5}$$

The absolute value of $\Delta U_{i,a}$ will be maximum when the voltage of phase *a* is maximum or minimum at node *i,* which means $|\Delta U_{i,a}|_{\max} = |U_{i,a} - U_{\text{rate,AC}}|$. Therefore, (5) can be converted to

$$\Delta U_{i,a} = k_1(\Delta U_{i,b} + \Delta U_{i,c}) + k_2 U_{\text{rate,AC}}, \tag{6}$$

where k_1 and k_2 are the correlation coefficients. If the voltage of phase *a* is maximum, $k_1 = (VU_{i,a} + 1)/(2 - VU_{i,a})$ and $k_2 = (3\times VU_{i,a})/(VU_{i,a} + 1)$. If the voltage of phase *a* is minimum, $k_1 = (1 - VU_{i,a})/(VU_{i,a} + 2)$ and $k_2 = (3\times VU_{i,a})/(VU_{i,a} + 2)$.

The coupling between voltage violation and unbalance can be mathematically described through (6).

Furthermore, the $VU_{i,a}$ is set as the limit value of 2% and is substituted into (6) to further quantify the coupled relation

mentioned above. Therefore, an analytical model of three-phase voltage deviations considering voltage violation and unbalance can be represented as follows (the derivation retains four decimal digits):

1) When $U_{i,a}$ is maximum at node i,

$$\Delta U_{i,a} \approx 0.5151(\Delta U_{i,b} + \Delta U_{i,c}) + 0.0303 . \quad (7)$$

In this case, the three-phase voltage deviation of node i should meet the constraint

$$\Delta U_{i,a} \geq 0.5\left|(\Delta U_{i,b} + \Delta U_{i,c})\right| . \quad (8)$$

2) When $U_{i,a}$ is minimum at node i,

$$\Delta U_{i,a} \approx 0.4851(\Delta U_{i,b} + \Delta U_{i,c}) - 0.0297 . \quad (9)$$

In this case, the three-phase voltage deviation of node i should meet the constraint

$$\Delta U_{i,a} < 0.5\left|(\Delta U_{i,b} + \Delta U_{i,c})\right| . \quad (10)$$

To facilitate analysis, it is assumed that over-voltage only occurs in phase a, thus the sum of the voltage deviations of phases b and c ($\Delta U_{i,b}$+$\Delta U_{i,c}$) satisfies (11).

$$\left|\Delta U_{i,b} + \Delta U_{i,c}\right| \leq 0.14 . \quad (11)$$

If $U_{i,a}$ is the maximum voltage of the three phases at node i, the coupling between single-phase voltage violation and voltage unbalance will be illustrated in Fig. 3(a), according to (7), (8), and (11) . If $U_{i,a}$ is the minimum voltage of the three phases at node i, the coupled relation will be shown in Fig. 3 (b), according to (9), (10), and (11).

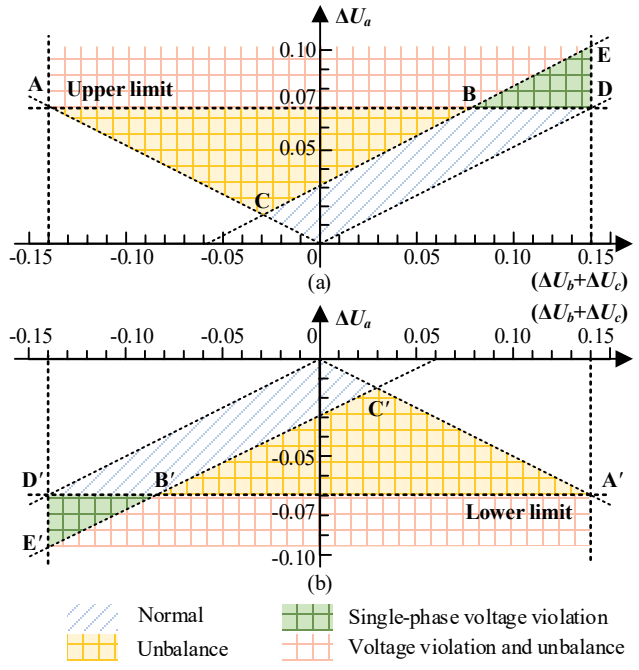

Fig. 3. A graph of the coupling between the voltage violation and unbalance. (a) The voltage of phase a is maximum at node i; (b) the voltage of phase a is minimum at node i.

The feasible regions in Fig. 3 are further divided into four subregions, considering the constraints of voltage deviation and unbalance issues:

1) **The blue subregion:**
   AC LVDNs operate normally.
2) **The yellow subregion:**
   Only three-phase voltage unbalance occurs in AC LVDNs.
3) **The green subregion:**
   Only single-phase voltage deviation occurs in AC LVDNs.
4) **The red subregion:**
   Voltage deviation and unbalance occur simultaneously in AC LVDNs.

It should be noted that the phase with the maximum voltage deviation can be different from the phase with the maximum $VU_{i,\varphi}$ at node i. However, The method proposed in this paper is still applicable because this approximation assumes that the two phases are the same and therefore has little effect on the regulation results.

Based on the graph shown in Fig. 3, the voltage violation and/or voltage unbalance in LVDNs can be easily known through the three-phase voltage deviations obtained from the voltage measurement at any nodes.

B. Voltage Adjustment Calculation Method under Different Voltage Violation Scenarios

In this section, a graph-based calculation method of voltage regulation requirements considering coupled voltage violation and unbalance is developed, according to Fig. 4.

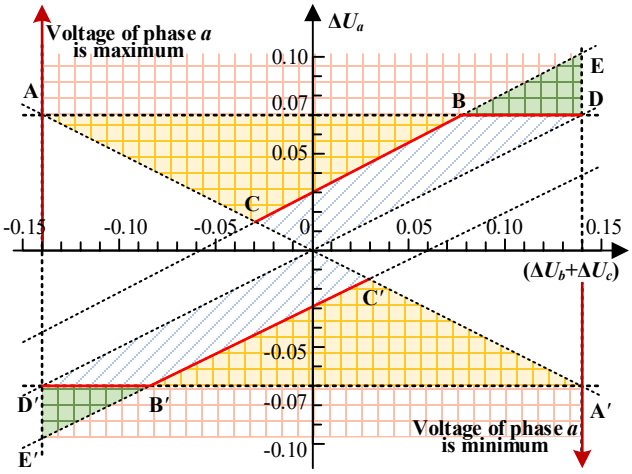

Fig. 4. A graph for voltage regulation requirement calculation.

Three voltage violation scenarios are divided in LVDNs for the convenience of discussion: single-phase voltage violation, two-phase voltage violation and three-phase voltage violation.

1) **Single-phase voltage violation:**
   If only one phase voltage exceeds the upper limit at node i, it will be discussed in the following three cases according to Fig. 4.
   a) Case 1– Over-voltage in phase a occurs as in Green regions (BDE): the minimum voltage regulation can be calculated through the red control curves BD.
   b) Case 2– Voltage unbalance occurs as in Yellow regions (ABC): the minimum voltage regulation can be calculated through (8) which is the red control curve BC.
   c) Case 3– Over-voltage and unbalance occur simultaneously in phase a as in Red regions (ABE): the minimum voltage regulation can be calculated through the red control curve CBD.

   When phase a voltage exceeds the lower limit, the voltage

regulation will be calculated through the red control curves marked with a prime in the negative Y-axis.

2) **Two-phase voltage violation:**
When extreme voltage violations of two phases at node *i* occur, the voltage of one phase will be firstly regulated to the voltage limit no matter whether there is voltage unbalance or not. Then the regulation requirement can be determined by the first scenario because the two-phase voltage violation will be turned into a single-phase voltage violation.

3) **Three-phase voltage violation:**
When extreme voltage deviation of the three-phase at node *i* exceeds the voltage limit, it can be discussed as the following two cases:

a) Case 1– All the three-phase voltages exceed the upper or lower limit: for example, if they exceed the upper limit, the three-phase voltages will be adjusted to the upper voltage limit 1.07 p.u., as shown at point D in Fig. 4. On the contrary, other situations will be opposite which the three-phase voltages will be adjusted to the lower limit 0.93 p.u., as shown at point D′ in Fig. 4. The *VU* in LVDNs will be 0 % after doing this.

b) Case 2– The three phases experience both over-voltage and under-voltage: there will be a serious unbalance if regulate the three-phase voltages to the limits as in Case 1, (point A or A′). Therefore, if phase *a* voltage exceeds the lower limit and the voltages of phases *b* and *c* exceed the upper limit, the voltages of phases *b* and *c* will be adjusted to the upper limit 1.07 p.u. and the voltage regulation of phase *a* will be calculated by (9), the regulation result will be at point C′ as shown in Fig. 4.

The graph-based voltage regulation calculation method for different voltage violation scenarios in LVDNs is summarized in Fig. 5, based on which the voltage adjustment can be easily calculated. Moreover, the voltage violation and unbalance at one node can be solved simultaneously by adjusting the devices only once or twice.

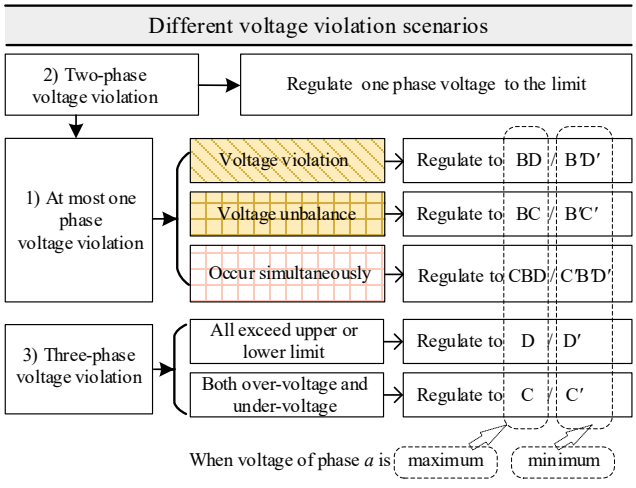

Fig. 5. Flowchart of the proposed graph-based voltage regulation calculation method.

IV. Coordinated Power Regulation Method for Three-Phase Four-Wire Hybrid AC/DC LVDNs

A. Partition Method Considering Both Active and Reactive Power

The target of partition is to choose the most efficient regulation devices for each node in hybrid AC/DC LVDNs. The electrical coupling between nodes is strong within the sub-areas but weak across sub-areas. Therefore, if the power of devices in a sub-area is adjusted, it will have a great impact on node voltages within its area but little impact on adjacent sub-areas. In other words, for the partitioning optimization method, strong coupling within the sub-areas and weak coupling across sub-areas should be guaranteed [26].

Objective Function

Electrical distance is a measure of the relative variation in voltage magnitudes between two nodes resulting from an alteration in active or reactive power injection at one of the nodes. In this way, the electrical coupling between two nodes can be established by observing the attenuation of voltage variations at nodes *i* and *j* as follows:

$$\Delta U_i = \alpha_{ij} \Delta U_j , \tag{12}$$

where α_{ij} is the interrelationship of voltage variation between nodes *i* and *j* in AC/DC LVDNs. It should be noted that both active and reactive power affect the voltage in AC LVDNs. Therefore, an equivalent coefficient γ_{ij} is developed for converting the active power to virtual reactive power. The parameters α_{ij} of AC side and DC side LVDNs can be obtained through (13) and (14).

$$\alpha_{ij}^{\mathrm{AC}} = \sum_{\varphi \in a,b,c} \frac{\Delta U_{i,\varphi}}{\Delta U_{j,\varphi}} = \sum_{\varphi \in a,b,c} \frac{\gamma_{ij,\varphi} S_{ij}^{\mathrm{AC},vp} + S_{ij}^{\mathrm{AC},vq}}{\gamma_{jj,\varphi} S_{jj}^{\mathrm{AC},vp} + S_{jj}^{\mathrm{AC},vq}} , \tag{13}$$

$$\alpha_{ij}^{\mathrm{DC}} = \frac{\Delta U_i}{\Delta U_j} = \frac{S_{ij}^{\mathrm{DC},vp}}{S_{jj}^{\mathrm{DC},vp}} , \tag{14}$$

where $S_{ij}^{\mathrm{AC},vp}$ and $S_{ij}^{\mathrm{AC},vq}$ are active power-voltage sensitivity and reactive power-voltage sensitivity of AC LVDNs, and γ_{ij} is the ratio of them [22]. $S_{ij}^{\mathrm{DC},vq}$ is the active power-voltage sensitivity of DC LVDNs.

To obtain symmetrical distances, (15) is taken as the definition of the electrical distances between nodes *i* and *j* at LVDNs:

$$D_{ji} = D_{ij} = -\lg\left(\alpha_{ij}\alpha_{ji}\right). \tag{15}$$

Considering the three-phase four-wire configuration, the first objective of the proposed partitioning optimization model is to minimize the product of maximum electrical distances in *n* sub-areas. In this case, the differences in the regulation efficiency between sub-areas can be reduced, which can be explained as:

$$f_1 = \min \prod_{n=1}^{N} D_{n,\max} , \tag{16}$$

where $D_{n,\max}$ is the maximum electrical distance between the nodes with devices and other nodes in the *n*-th sub-area. The smaller the electrical distance between nodes, the higher the efficiency of device regulation [27], [28]. *N* is the number of partitions.

The second objective is to minimize the total squares of deviations of real and reactive power reserves considering both

regulation capacity and cost.

$$f_2 = \min \sum_{n=1}^{N} (R_n - \overline{R})^2, \tag{17}$$

where R_n is the power reserve of real and reactive power in partition n. $\overline{R}$ is the average power reserve of hybrid AC/DC LVDNs.

The power reserves R_n in AC and DC partitions can be calculated according to (18) and (19), which considers both maximum regulation capacities, cost of regulation devices and voltage requirements of each partition.

$$R_n^{\mathrm{AC}} = \frac{\sum_{t=1}^{v} C_t P_{n,t}^{CD} \cdot \sum_{i=1}^{w} S_{i,t}^{\mathrm{AC},vp} + \sum_{t=1}^{v} C_t Q_{n,t}^{CD} \cdot \sum_{l=1}^{w} S_{i,t}^{\mathrm{AC},vq}}{\sum_{i=1}^{w} \sum_{\varphi \in a,b,c} \Delta U_{i,\varphi}}, \tag{18}$$

$$R_n^{\mathrm{DC}} = \frac{\sum_{t=1}^{v} C_t P_{n,t}^{CD} \cdot \sum_{i=1}^{w} S_{i,t}^{\mathrm{DC},vp}}{\sum_{i=1}^{w} \Delta U_i}, \tag{19}$$

where v and w are the number of controllable devices and the number of nodes in partition n. C_t is the regulation cost per unit power of controllable devices. $P_{n,t}^{CD}$ and $Q_{n,t}^{CD}$ are active and reactive power capabilities of controllable devices in partition n. If the ratio R_n is greater than or equal to 1, the total regulation capacity of the devices considering power regulation cost can meet the demand of voltage regulation, and the power in this sub-area will be sufficient. If the ratio R_n is less than 1, the power regulation capacity in this sub-area will be insufficient.

Constraints

The ratings of the controllable devices are considered as the constraints of the partitioning optimization method:

$$\left(P_{\varphi}^{\mathrm{CD}}\right)^2 + \left(Q_{\varphi}^{\mathrm{CD}}\right)^2 = \left(S_{\varphi}^{\mathrm{CD}}\right)^2, \tag{20}$$

where $S_{\varphi}^{\mathrm{CD}}$ represents the single-phase rated capacity of PVs, ESSs, or VSCs, and the active power of VSCs also needs to meet the constraint:

$$\sum_{\varphi \in (a,b,c)} \left| P_{\varphi}^{\mathrm{AC,VSC}} \right| = \left| P^{\mathrm{DC,VSC}} \right| + P_{loss}^{\mathrm{VSC}}, \tag{21}$$

where P_{loss}^{VSC} is the power loss of VSCs and is 2% of the rated capacity. $P_{\varphi}^{\mathrm{AC,VSC}}$ and $P^{\mathrm{DC,VSC}}$ are the active power of VSCs on the AC side and DC side.

B. Sensitivity-Based Voltage Regulation Method

A partition-based coordination strategy is developed considering the three-phase four-wire sensitivities in hybrid AC/DC LVDNs. The coordinated voltage control strategy will be triggered if voltage violation and voltage unbalance occurred.

Sensitivities of hybrid AC/DC LVDNs with three-phase four-wire topology

The ABCD parameters-based sensitivity calculation method is adopted in this paper considering the three-phase four-wire topology of hybrid AC/DC LVDNs [8]. The voltage sensitivities at node j due to the injected active and reactive power at node i are:

$$S_{ji}^{vp} = -\sum_{l \in \left(C_{0,i} \cap C_{0,j}\right)} R_l / U_{\mathrm{rate}}, \tag{22}$$

$$S_{ji}^{vq} = -\sum_{l \in \left(C_{0,i} \cap C_{0,j}\right)} X_l / U_{\mathrm{rate}}, \tag{23}$$

where $C_{i,j}$ is the set of all lines between nodes i and j. R_l and X_l are the equivalent resistance and reactance of the power distribution lines l, which can be calculated through ABCD parameters considering the three-phase four-wire topology on the AC side. The size of the S_{ji}^{vp}, S_{ji}^{vq}, R_l, and X_l matrices is 4×4.

The positions and phases of the nodes will affect the sensitivity calculation as shown in Fig. 6. x ($x \in \{a, b, c, n\}$) and v ($v \in \{a, b, c, n\}$) ($x \neq v$) are used to describe the phases of the two selected nodes.

In a three-phase four-wire line model, the ABCD parameters are the coefficients in the relationship between the voltage and current of two nodes calculated through Kirchhoff's Current and Voltage Laws [8], [29]. The ABCD parameter-based calculations of R_l and X_l are developed in the following two scenarios as shown in Fig. 6.

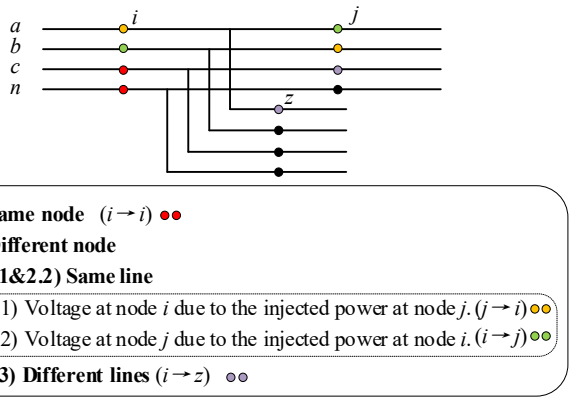

Fig. 6. Positions and phases of the selected nodes in a radial LVDN.

The calculations of R_l and X_l are developed in the following two scenarios as shown in Fig. 6:

$$\sum R_l = \begin{cases} Re(\left[B_j\right]_{v,x}) & \text{, if case 1} \\ Re\left[A_{ij}\left[B_j\right]_{cx}\right]_{rv} & \text{, if case 2.1} \\ Re\left[a_{ij}\left[B_j\right]_{cx} + \left[B_{ij}\right]_{cx}\right]_{rv} & \text{, if case 2.2} \\ Re\left[A_{yz}(a_{yj}\left[B_j\right]_{cx} + \left[b_{yj}\right]_{cx})\right]_{rv} & \text{, if case 2.3} \end{cases}, \tag{24}$$

$$\sum X_l = \begin{cases} Re(\left[B_j\right]_{v,x}) & \text{, if case 1} \\ Re\left[A_{ij}\left[B_j\right]_{cx}\right]_{rv} & \text{, if case 2.1} \\ Re\left[a_{ij}\left[B_j\right]_{cx} + \left[B_{ij}\right]_{cx}\right]_{rv} & \text{, if case 2.2} \\ Re\left[A_{yz}(a_{yj}\left[B_j\right]_{cx} + \left[b_{yj}\right]_{cx})\right]_{rv} & \text{, if case 2.3} \end{cases}, \tag{25}$$

where $[B_j]_{cx}$ is the element in column x of matrix B_j and $[B_j]_{rv}$ is the element in row v of matrix B_j. The size of the A, B, a, and b matrices is 4×4.

The ABCD parameter calculation method is also applicable to DC distribution networks. The reactive power-voltage sensitivity S^{vq} of the DC side will be set as zero because there is no reactance of DC lines.

Thus, the active and reactive power adjustment of

controllable devices can be obtained through sensitivity from (26) and (27):

$$\Delta P = \Delta U / S^{vp}, \tag{26}$$

$$\Delta Q = \Delta U / S^{vq}. \tag{27}$$

It should be mentioned that the active and reactive power of ESSs, VSCs and PVs can be independently controlled, and the ABCD sensitivity can be utilized for both AC and DC sides.

The changes in active and reactive power of different nodes have a superimposed impact on node voltage, therefore the voltage variation of any node during the coordinated control of active and reactive power of the controllable devices will be satisfied [30]:

$$\Delta U = \sum S^{vp} \Delta P + \sum S^{vq} \Delta Q. \tag{28}$$

Coordination strategy

1) On the AC side

The voltage regulation requirements will be calculated as shown in Fig. 4 if a voltage violation or voltage unbalance occurs. The first priority is to regulate the reactive power of PV inverters in the same partition when PV capacity is still available. The active and reactive power of PV should meet the constraint of DG's capacity and the adjustment of ΔQ^{PV} is obtained through (30).

$$Q_{\varphi}^{\mathrm{PV}} = \pm\sqrt{\left(S^{\mathrm{inv}}\right)^2 - \left(P_{\varphi}^{\mathrm{PV}}\right)^2}, \tag{29}$$

$$\Delta Q_{i,\varphi} = \Delta U_{i,\varphi} / S^{\mathrm{AC},vq}, \tag{30}$$

where S^{inv} is the rated capacity of DG, P^{PV} is the active power of DG and ΔQ should not exceed P^{PV}.

Secondly, if the reactive power adjustment cannot be achieved due to the power rating limit of PV, the ESSs or VSCs in the same partition will be considered to regulate the voltage. For VSCs, the reactive power is firstly considered to regulate the voltage because the DC line is not affected by the reactive power regulation on the AC side. The reactive power adjustment ΔQ^{VSC} can be calculated by (30). For ESSs, the active power is firstly adjusted to regulate the voltage to avoid the curtailment of PVs, and the active power adjustment ΔP^{ESS} can be obtained from:

$$\Delta P = \Delta U_{i,\varphi} / S^{\mathrm{AC},vp}. \tag{31}$$

If the VSCs' reactive capacity or ESSs' active power capacity is insufficient when alleviating AC side voltage violation, both active and reactive power will be used to coordinate and regulate node voltages:

$$\begin{cases} \Delta U_{i,,\varphi} = S^{\mathrm{AC},vp} \cdot \Delta P_{i,\varphi}^{\mathrm{AC}} + S^{\mathrm{AC},vq} \cdot \Delta Q_{i,\varphi}^{\mathrm{AC}} \\ \left(P^{\mathrm{AC}} + \Delta P^{\mathrm{AC}}\right)^2 + \left(Q^{\mathrm{AC}} + \Delta Q^{\mathrm{AC}}\right)^2 = S^{CD2} \end{cases}. \tag{32}$$

DC voltage variation will occur when the active power regulation on the AC side changes. Therefore, the absolute value of ESSs' or VSCs' active power will be reduced to release the reactive power capacity, considering reducing the active power regulation effect on the DC side.

Finally, if LVDNs still have voltage violation or voltage unbalance after the adjustment of PVs, ESSs, and VSCs, the curtailment of PVs in the same partition will be proposed to maintain normal voltage on the AC side. ΔP^{PV} and ΔQ^{PV} can be calculated through (32).

2) On the DC side

If a DC voltage exceeds the limits, the active power of VSCs or ESSs in the same partition will be primarily adjusted to regulate node voltages according to (31). If the active capacity is insufficient, equation (32) will be used to achieve the coordinated control of active power and reactive power so as to solve voltage violation. The absolute value of active power (ΔP^{VSC} or ΔP^{ESS}) will be released as could as possible by reducing reactive power (ΔQ^{VSC} or ΔQ^{ESS}). And the curtailment of PV will be adopted when voltage violation is not solved completely through all the above methods.

The flowchart of the proposed sensitivity-based coordination control method for voltage violation and voltage unbalance in hybrid AC/DC LVDNs is shown in Fig. 7.

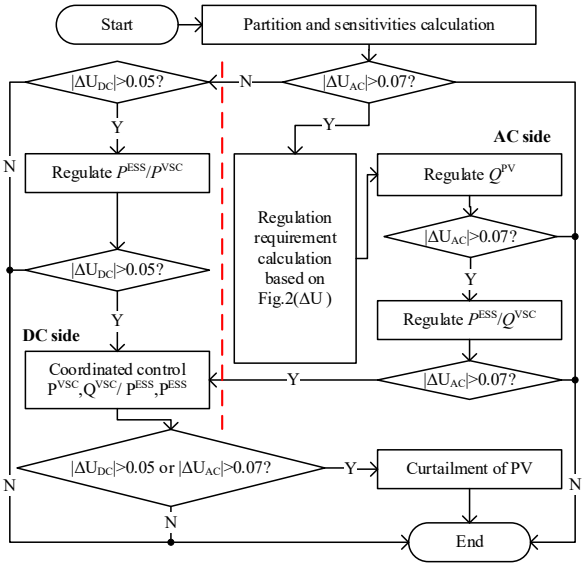

Fig. 7. Flowchart of proposed coordination control method.

V. Algorithm

Optimal partition results are obtained through a standard genetic algorithm, and the optimization model is as follows

$$\begin{cases} obj = \min\left(f_1 / F_1 + f_2 / F_2\right) \\ \text{s.t. (20) and (21)} \end{cases}. \tag{33}$$

In (33), f_1 and f_2 are the objective functions, including (12)-(16) and (17)-(19) respectively. f_1 and f_2 divided by F_1 and F_2 are to normalize the dimension. The ΔU_i in (18) and (19) is the maximum voltage regulation requirement of each partition, which can be obtained from the worst scenario of the day based on the graph method proposed in Section III.

Using binary encoding and each line (l) in hybrid AC/DC LVDNs is represented by a gene (g_l) to ensure the connectivity of partition. These genes form a chromosome:

$$g = (g_1, g_2, g_3, \ldots, g_l). \tag{34}$$

If the two nodes of line l are within the same partition, g_l will be 0, otherwise, g_l will be 1.

VI. Case Study

A. Simulation Conditions

A 30-node hybrid AC/DC LVDN embedded with PVs and ESSs, as shown in Fig. 7, is used to verify the proposed method. The DC line denoted by the red line and the AC line, which is represented by the black line, are modified by [24]. The typical profiles of PV output and load for a 24-hour period are given in [24]. Details of the network parameters and load data can be found in [24] as well. The rated power of single-phase PV generation is 3 kW and the rated power of ESS is 5 kWh which is connected to the distribution network in three-phase and can be adjusted in a single phase. The rated capacity of VSC2 is 20 kW. The voltages on the secondary side of distribution transformers are fixed as 1.0 p.u. The penetration of PVs in this study is 127.07%.

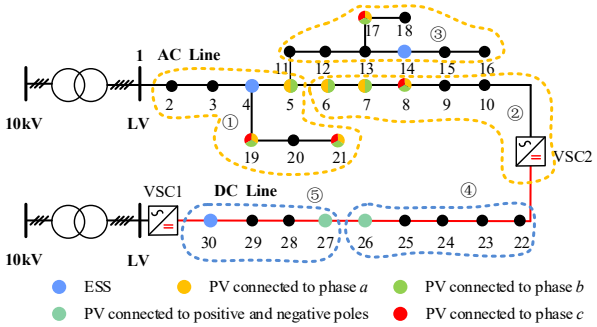

Fig. 8. A single-line diagram hybrid AC/DC LVDN integrated with PVs and ESSs.

B. Study-1 Partition Method

In Result 1, the partition method only considers the reactive power capability in electrical distance calculation. In Result 2, the equivalence of real power to reactive power is considered in the proposed partition method.

TABLE I
Partitioning Results for Different Partition Methods

Methods	Partition results	Regulation efficiency	Regulation capacity and cost
Result 1	[2-7,19-21], [8-10], [11-18], [22-25], [26-30]	0.67	0.45
Result 2	[2-5,19-21], [6-10], [11-18], [22-26], [27-30]	0.35	0.31

Fig. 8 illustrates the partitioning results of the proposed method in Result 2. For the AC side, nodes 6 and 7 are assigned to Area 2 in Result 2 and Area 1 in Result 1 due to the lower cost of PVs compared with VSC2. Moreover, VSC2 has sufficient active power regulation capacity to satisfy the high voltage regulation requirement in Area 2.

For the DC side, node 26 is in Area 4 in Result 2 and in Area 5 in Result 1, as shown in Table I. Due to the considerable rated capacity of VSC2, the active power regulation capacity of VSC2 is higher than the ESS at node 30. Therefore, the regulation effect of Result 2 is better than Result 1 because the electrical distance from node 26 to Area 4 equals the distance to Area 5 and the comparable adjustment costs of VSC2 and ESS.

C. Study-2 Voltage Control Method for Solving Voltage Violation and Unbalance Simultaneously

Cases 0 to 3 represent scenarios employing different control strategies, whereas Case 4 is characterized by the implementation of the sensitivity-based control strategy proposed in this paper.

Case 0: Without control.

Case 1: Based on the priority-based voltage control method, the voltage unbalance will be solved first and then the voltage violation [8].

Case 2: Solve the voltage violation with PVs and ESSs and eliminate voltage unbalance with VSC2 simultaneously.

Case 3: Solve the two issues simultaneously based on partitioning Result 1.

Case 4: Solve the two issues simultaneously based on partitioning Result 2 of the proposed partition method.

In Case 0, the distribution network on the AC side has serious voltage violation and unbalance during the day, as shown in Fig. 9. The two issues occur simultaneously from 10:00 to 16:00. The voltage of phase *a* at node 8 reaches the peak at 13:00, which is 1.1064 p.u. At this time, the maximum *VU* is 2.71% at node 9 of phase *c*.

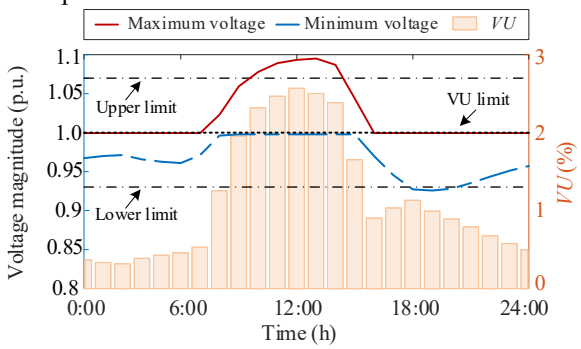

Fig. 9. Maximum voltages and *VU*s on the AC side in 24 hours.

In Case 1, the overvoltages at nodes 5 to 18 become worse and the three-phase voltages all exceed the upper limit after managing voltage unbalance first, as shown in Fig. 10(b). It is because that the average voltage of node 9 is greater than 1.07 p.u., which causes the voltages of both phases *a* and *b* to be too high to exceed the limit. Implementing the prioritized control method to regulate the voltages to their average value (1.0879 p.u.) can mitigate the unbalance. As illustrated in Fig. 11, the *VU* of Case 1 has been regulated as the minimum. However, it results in overvoltage in phase *c*, as indicated in Fig. 10(b). Although subsequent voltage control measures can stabilize the operation of the LVDN, regulating the voltage of phase *c* brings unnecessary device interventions, which will diminish their lifespan.

In Case 2, PVs absorb reactive power to reduce the voltages of phases *a* and *b* at node 8 at 13:00. The ESS at node 4 further enhances the voltages of phases *a* and *b* by being charged when the capacity of PV is insufficient. At the same time, to alleviate the three-phase unbalance at node 9, VSC2 outputs the reactive power of phase *c* and absorbs the reactive power of phases *a* and *b*, as depicted in Fig. 12. However, the voltages of node 8 are overregulated due to the superposition of the regulation effect of ESS and VSC. Therefore, there are still voltage violation and unbalance at nodes 7 to 10. Iteration of "voltage measurement and regulation" in Case 2 is needed to solve the

two issues simultaneously, and the iteration result is shown in Fig. 10(c).

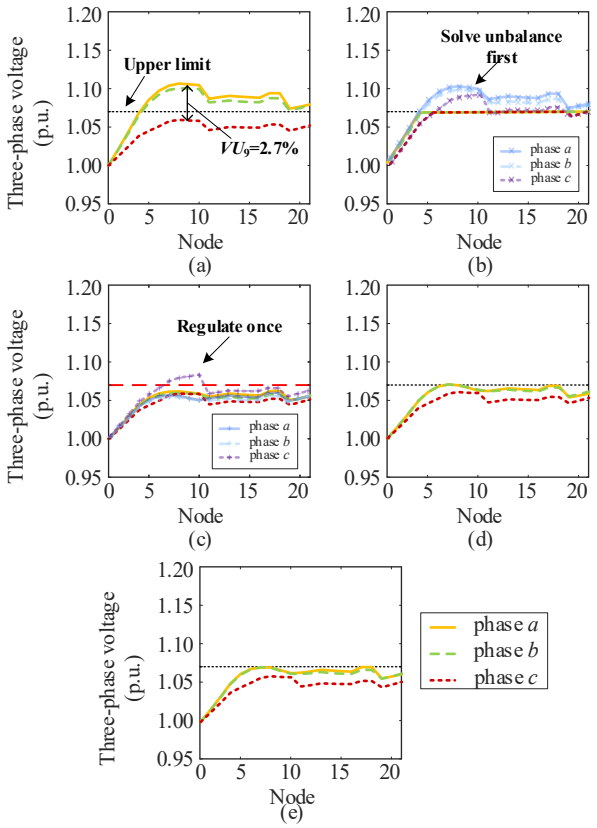

Fig. 10. Three-phase voltages on the AC side at 13:00. (a) Case 0; (b) Case 1; (c) Case 2; (d) Case 3; (e) Case 4.

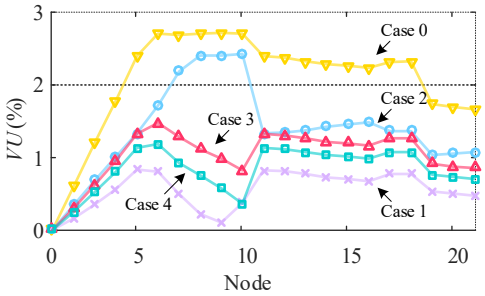

Fig. 11. *VUs* of different cases at 13:00.

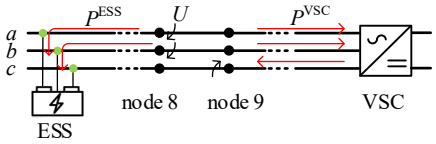

Fig. 12. Directions of the regulated power at 13:00 for Case 2.

Case 3 and Case 4 have similar effects on voltage regulation, as shown in Figs. 10(d) and (e). Fig. 13 shows the power management of the controllable devices in Cases 3 and 4. When the voltage of node 8 reaches 1.10 p.u. at 11:00 in Case 4, the reactive power of PVs at nodes 6, 7, and 8 cannot control the voltage back to 1.07 p.u. Thus, the reactive power of VSC2 is utilized for voltage improvement according to (27). However, the reactive power of VSC and PV in Area 2 is insufficient in Case 3. Therefore, the active power of VSC is reduced to increase the reactive power capacity according to (32). When the power output of PVs reaches its peak at 13:00, VSC2 reduces its active power to give more regulation capacity for increasing reactive power absorbed from the AC lines in Case 4. Although both active and reactive power is coordinated and regulated, the VSC cannot control the voltage back to 1.07 p.u. due to the limited regulation capacity in Case 3. Therefore, the curtailment of about 1.66 kWh of PVs is triggered to mitigate the overvoltages on the AC side.

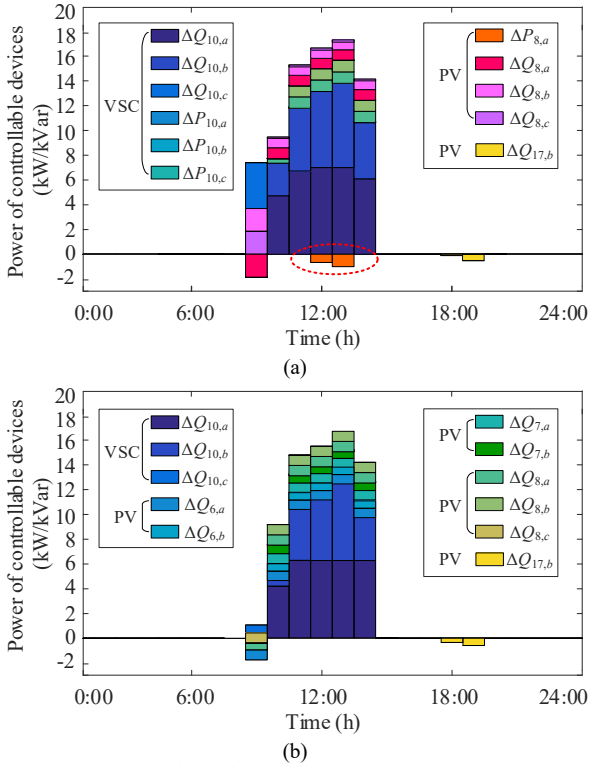

Fig. 13. Power of controllable devices for Cases 3 and 4. (a) Case 3; (b) Case 4.

The regulation costs of ESS, VSC, and PV are shown in Table II. The regulation cost in Case 3 exceeds the cost in Case 4 by \$2.4368, due to the high curtailment cost of PVs in Table III. Moreover, in Case 4, the inclusion of PVs at nodes 6 and 7 within Area 2 leads to a reduction in the output of VSC2. This leads to a further reduction in the total expense in Case 4 due to the cost-effectiveness of PV reactive power regulation.

TABLE II
REGULATION COSTS FOR DIFFERENT DEVICES

Devices	Active power regulation (\$/kWh)	Reactive power regulation (\$/kVarh)
PV	0.3127 (curtailment)	0.0094
ESS	0.0819	0.0104
VSC	0.1941	0.0345

TABLE III
ADJUSTMENT COSTS (\$) FOR CASES 3 AND 4

Cost	Case 3	Case 4
The curtailment of PV	0.5175	0
Reactive power regulation of PV	0.0863	0.1617
Active power regulation of VSC	1.5095	0
Reactive power regulation of VSC	2.4691	1.9731
Total cost	4.5716	2.1348

D. Study-2 Coordinated Control Method Based on Three-Phase Four-Wire Sensitivity

The "Perturb-and-observe" sensitivity calculation method, the three-phase three-wire sensitivity calculation method

without considering the effect of the neutral line and the three-phase four-wire sensitivity calculation method presented in this paper are used to calculate the sensitivities of AC LVDNs. Voltage qualified rate (VQR) is used to represent the control efficiency in different cases, and the comparison of different sensitivity calculation methods is shown in Table IV. The first method with the highest accuracy is taken as a comparative example.

TABLE IV
COMPARISON OF CONTROL RESULTS BASED ON DIFFERENT SENSITIVITY CALCULATION METHODS

Sensitivity calculation methods	VQR(%)	Time(s)
Perturb-and-observe	100%	0.2536
Three-phase three-wire	98.68%	0.1725
Three-phase four-wire	99.80%	0.1976

Results show that the calculation time of the three-phase four-wire sensitivity calculation method is 0.0251s longer than that of the three-phase three-wire sensitivity calculation method. The calculation time of the "Perturb-and-observe" sensitivity calculation method is the longest because it requires cyclic power flow calculation for several times.

The difference between the control strategy based on the sensitivity considering the influence of the neutral line and the control result of the comparison example is the smallest, the VQR difference is 0.20%. The accuracy of the proposed method is higher than that of the control method based on three-phase three-wire sensitivity, and the VQR is 1.12% higher than it.

VII. CONCLUSION

This paper proposed a partition-based regulation method for managing voltage violation and voltage unbalance simultaneously in three-phase four-wire hybrid AC/DC LVDNs with high penetration of PVs. Unlike the existing priority-based voltage control strategy, the proposed method considers the coupling between voltage violation and unbalance and describes it using a graph based on the three-phase analytical model. The proposed graph visualizes the coupling of the two issues clearly with different subregions and is used to calculate the voltage adjustment for solving the two issues simultaneously. This method is also superior to the existing partition-based regulation method since the electrical distance calculation considers the regulation capability of active power and the three-phase structure, which is more suitable for hybrid AC/DC LVDNs to determine controllable devices in each part. Moreover, the proposed three-phase four-wire sensitivity-based coordinated control method fulfills the speed requirement and enhances accuracy for voltage management. The performance of the proposed voltage control strategy has been demonstrated using a real 24-hour load profile on an unbalanced test hybrid AC/DC LVDNs.

REFERENCE

[1] B. Liu, K. Meng, Z. Y. Dong, P. K. C. Wong and X. Li, "Load Balancing in Low-Voltage Distribution Network via Phase Reconfiguration: An Efficient Sensitivity-Based Approach," *IEEE Trans. Power Del*, vol. 36, no. 4, pp. 2174-2185, Aug. 2021.

[2] F. Bai, R. Yan, T. K. Saha and D. Eghbal, "An Excessive Tap Operation Evaluation Approach for Unbalanced Distribution Networks with High PV Penetration," *IEEE Trans. Sustain. Energy*, vol. 12, no. 1, pp. 169-178, Jan. 2021.

[3] Y. Cai, W. Tang, L. Zhang and O. Xu, "Multi-mode voltage control in low distribution networks based on reactive power regulation of photovoltaic inverters," *Automation of Electric Power Systems*, vol. 41, no. 13, pp. 133-141, Nov. 2017.

[4] W. Jiao, J. Chen, Q. Wu, C. Li, B. Zhou and S. Huang, "Distributed Coordinated Voltage Control for Distribution Networks with DG and OLTC Based on MPC and Gradient Projection," *IEEE Trans. Power Syst*, vol. 37, no. 1, pp. 680-690, Jan. 2022.

[5] A. Bedawy, N. Yorino, K. Mahmoud, Y. Zoka and Y. Sasaki, "Optimal Voltage Control Strategy for Voltage Regulators in Active Unbalanced Distribution Systems Using Multi-Agents," *IEEE Trans. Power Syst*, vol. 35, no. 2, pp. 1023-1035, March. 2020.

[6] M. Zeraati, M. E. H. Golshan and J. M. Guerrero, "Voltage Quality Improvement in Low Voltage Distribution Networks Using Reactive Power Capability of Single-Phase PV Inverters," *IEEE Trans. Smart Grid*, vol. 10, no. 5, pp. 5057-5065, Sept. 2019.

[7] X. Xiao, Z. Li, Y. Wang, Y. Zhou and K. Liu, "Optimal Power Quality Compensation of Energy Storage System in Distribution Networks Based on Unified Multi-Phase OPF Model," *IEEE Trans. Smart Grid*, vol. 13, no. 3, pp. 1873-1887, May. 2022.

[8] L. Zhang, C. Zhao, B. Zhang, G. Li and W. Tang, "Voltage control method based on three-phase four-wire sensitivity for hybrid AC/DC low-voltage distribution networks with high-penetration PVs," *IET Renew. Power Gen.*, vol. 16, no. 4, pp. 700-712, Mar. 2022.

[9] X. Su, M. A. S. Masoum and P. J. Wolfs, "Optimal PV Inverter Reactive Power Control and Real Power Curtailment to Improve Performance of Unbalanced Four-Wire LV Distribution Networks," *IEEE Trans. Sustain. Energy*, vol. 5, no. 3, pp. 967-977, July. 2014.

[10] Zeraati, M., M.E.H. Golshan and J.M. Guerrero, "Voltage Quality Improvement in Low Voltage Distribution Networks Using Reactive Power Capability of Single-Phase PV Inverters," *IEEE Trans. Smart Grid*, vol. 10, no. 5, pp. 5057-5065, Mar. 2019.

[11] T. Dimitrios, D. Gaspard, D. Olivier,G. Konstantinos N and L. Christos S, "An integrated tool for optimal energy scheduling and power quality improvement of a microgrid under multiple demand response schemes," *Appl. Energy*, vol. 260, Feb. 2020.

[12] B. Zhang, W. Tang, Y. Cai, Z. Wang, T. Li and H. Zhang, "Distributed Control Strategy of Residential Photovoltaic Inverter and Energy Storage Based on Consensus Algorithm," *Automation of Electric Power Systems*, vol. 44, no. 2, pp. 86-94, Apr. 2020.

[13] J. Liao, N. Zhou, Y. Huang and Q. Wang, "Unbalanced voltage suppression in a bipolar DC distribution network based on DC electric springs," *IEEE Trans. Smart Grid*, vol. 11, no. 2, pp. 1667-1678, March. 2020.

[14] H.M.A. Ahmed, M.M.A. Salama, "Energy Management of AC-DC Hybrid Distribution Systems Considering Network Reconfiguration," *IEEE Trans. Power Syst*, vol. 34,no. 6, pp.4583-4594, Nov. 2019.

[15] P. Li, C. Zhang, Z. Wu, Y. Xu, M. Hu and Z. Dong, "Distributed Adaptive Robust Voltage/VAR Control With Network Partition in Active Distribution Networks," *IEEE Trans. Smart Grid*, vol. 11, no. 3, pp. 2245-2256, May 2020.

[16] P., Li, *et al*., "MPC-Based Local Voltage Control Strategy of DGs in Active Distribution Networks," *IEEE Trans. Sustain. Energy*, vol. 11, no. 4, pp. 2911-2921, Oct. 2020.

[17] K. Alzaareer, M. Saad, H. Mehrjerdi, D. Asber and S. Lefebvre, "Development of New Identification Method for Global Group of Controls for Online Coordinated Voltage Control in Active Distribution Networks," *IEEE Trans. Smart Grid*, vol. 11, no. 5, pp. 3921-3931, Sept. 2020.

[18] Y. Yang, Y. Sun, Q. Wang, F. Liu and L. Zhu, "Fast Power Grid Partition for Voltage Control with Balanced-Depth-Based Community Detection Algorithm," *IEEE Trans. Power Syst*, vol. 37, no. 2, pp. 1612-1622, March. 2022.

[19] L. Zhang, Y. Chen, C. Shen, W. Tang and J. Liang, "Coordinated voltage regulation of hybrid AC/DC medium voltage distribution networks," *J. Mod. Power Syst. Clean Energy*, vol. 6, no. 3, pp. 463-472, May. 2018.

[20] J. Ding, Q. Zhang, S. Hu, Q. Wang and Q. Ye, "Clusters partition and zonal voltage regulation for distribution networks with high penetration of PVs," *IET Gener. Transm. Dis.*, vol. 12, no. 22, pp. 6041-6051, Dec. 2018.

[21] Y. Chai, L. Guo, C. Wang, Z. Zhao, X. Du and J. Pan, "Network Partition and Voltage Coordination Control for Distribution Networks With High Penetration of Distributed PV Units," *IEEE Trans. Power Syst*, vol. 33, no. 3, pp. 3396-3407, May. 2018.

[22] H. Ruan, H. Gao, Y. Liu, L. Wang and J. Liu, "Distributed Voltage Control in Active Distribution Network Considering Renewable Energy: A Novel

Network Partitioning Method," *IEEE Trans. Power Syst*, vol. 35, no. 6, pp. 4220-4231, Nov. 2020.
[23] Y. Cai, W. Tang, L. Li, B. Zhang, L. Zhang, Y. Wang, "Multi-mode adaptive local reactive power control method based on PV inverters in low voltage distribution networks," *IET Gener. Transm. Dis.*, vol. 14, no. 4, pp. 542-551, Feb. 2020.
[24] W. Tang, T. Li, L. Zhang, Y. Cai, B. Zhang, Z. Wang, "Coordinated Control of Photovoltaic and Energy Storage System in Low-voltage Distribution Networks Based on Three-phase Four-wire Optimal Power Flow," *Automation of Electric Power Systems*, vol. 44, no. 12, pp. 31-42, Spet. 2020. (*in chinese*)
[25] W. E. Vanço, F. B. Silva and J. R. B. A. Monteiro, "A Study of the Impacts Caused by Unbalanced Voltage (2%) in Isolated Synchronous Generators," *IEEE Access*, vol. 7, pp. 72956-72963, May. 2019.
[26] Y. Lin, X. Lei, Q. Yang, J. Zhou, X. Chen, and J. Wen, "A distributed PageRank-based dynamic partition algorithm to improve distributed energy storages participation in frequency regulation," *Int. J. Electr. Power Energy Syst.*, vol. 150, pp. 105-109, Aug. 2023.
[27] P. Lagonotte, J. C. Sabonnadiere, J. Y. Leost, and J. P. Paul, "Structural analysis of the electrical system: application to secondary voltage control in France," *IEEE Trans. Power Syst.*, vol. 4, no. 2, pp. 479-486, Jan. 1989.
[28] Z. Lin, F. Tang, C. Yu, H. Li, L. Zhong, X. Wang, and H. Deng, "Reactive Power Compensation Strategy of the Electric Vehicle Connected to the Distribution Network in the Limit State Considering Voltage Constraint," *Sustainability*, vol. 15, no. 11, pp. 8634, May. 2023.
[29] W. H. Kersting, "Distribution System Modeling and Analysis", Boca Raton, FL, USA: CRC Press, vol. 1, 2002.
[30] K. H. Youssef, "A New Method for Online Sensitivity-Based Distributed Voltage Control and Short Circuit Analysis of Unbalanced Distribution Feeders," *IEEE Trans. Smart Grid*, vol. 6, no. 3, pp. 1253-1260, May. 2015.

Chunxue Zhao (Student Member, IEEE) was born in Tongliao, Inner Mongolia, China on May 20, 1998. She received the B.S. degree in electrical engineering from China Agricultural University, Beijing, China, in 2020. She is currently working toward the Ph.D. degree in agricultural electrification and automation at the College of Information and Electrical Engineering, China Agricultural University.

Her main research interests include hybrid AC/DC distribution network, power quality problem management, and voltage control of active distribution network.

Gen Li (Senior Member, IEEE) received the B.Eng. degree in Electrical Engineering from Northeast Electric Power University, Jilin, China, in 2011, the M.Sc. degree in Power Engineering from Nanyang Technological University, Singapore, in 2013 and the Ph.D. degree in Electrical Engineering from Cardiff University, Cardiff, U.K., in 2018.

He is now an Associate Professor in Power System at the Technical University of Denmark (DTU), Denmark. From 2013 to 2016, he has been a Marie Curie Early Stage Research Fellow funded by the European Commission's MEDOW project. He has been a Visiting Researcher at China Electric Power Research Institute and Global Energy Interconnection Research Institute, Beijing, China, at Elia, Brussels, Belgium and at Toshiba International (Europe), London, U.K. He was a Research Associate at the School of Engineering, Cardiff University from 2018 to 2022. His research interests include control and protection of HV and MV DC technologies, offshore wind, offshore energy islands, reliability modelling and evaluation of power electronics systems.

Dr. Li is a Chartered Engineer in the U.K., a Young Editorial Board Member of *Applied Energy*, an Associate Editor of the *CSEE Journal of Power and Energy Systems* and *IET Energy Systems Integration*, an Editorial Board Member of *CIGRE ELECTRA* and *Global Energy Interconnection* and an IET Professional Registration Advisor. His Ph.D. thesis received the First CIGRE Thesis Award in 2018. He is now a Committee Member of IEEE PES Denmark, the Academic Initiatives and Sub-committee Coordinator of IEEE PES Young Professionals, the Technical Panel Sectary of CIGRE U.K. B5 Protection and Automation and a Steering Committee Member of CIGRE Denmark NGN.

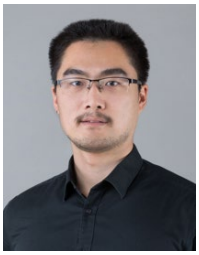

Lu Zhang (Senior Member, IEEE) was born in Beijing, China on February 10, 1990. He received the B.S. degree in electrical engineering and the Ph.D. degree in Agricultural Electrification and Automation from China Agricultural University, Beijing, China, in 2011 and 2016, respectively. He was a postdoc in the Department of Electrical Engineering at Tsinghua University From 2017 to 2019.

He is currently an Associate Professor at College of Information and Electrical Engineering, China Agricultural University, Beijing, China. His main research interests include hybrid AC/DC distribution network, renewable energy generation, and active distribution networks.

Dr. Zhang is a Young Editorial Board Member of Applied Energy, an Associate Editor of the CSEE Journal of Power and Energy Systems, an Academic Editor of Journal of System Simulation and Standing Director of IEEE PES DC Power System Satellite Committee-China, Low Voltage DC Technical Subcommittee.

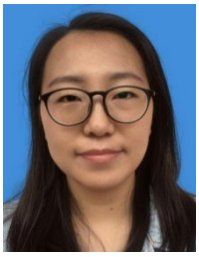

Bo Zhang (Member, IEEE) received the B.S. degree in electrical engineering and the Ph.D. degree in Agricultural Electrification and Automation from China Agricultural University, Beijing, China, in 2016 and 2022, respectively.

Her main research interests include hybrid AC/DC distribution network, renewable energy generation, and economic operation of active distribution network.

Wei Tang (Member, IEEE) received the B.S. degree in electrical engineering from Huazhong University of Science and Technology, Wuhan, China, in 1992 and the Ph.D. degree in electrical engineering from Harbin Institute of Technology, Harbin, China, in 1998. From 1998 to 2000, she was a post-doctor with Harbin Engineering University.

She is currently a professor at the College of Information and Electrical Engineering, China Agricultural University, Beijing, China. Her research interests include distribution network economic and security operation, distributed generation and active distribution network.